



Aberrant α -Adrenergic Hypertrophic Response in Cardiomyocytes from Human Induced Pluripotent Cells

Gabor Földes,^{1,2,*} Elena Matsa,³ János Kriston-Vizi,⁴ Thomas Leja,¹ Stefan Amisten,⁵ Ljudmila Kolker,^{1,6} Thusharika Kodagoda,¹ Nazanin F. Dolatshad,¹ Maxime Mioulane,¹ Karine Vauchez,¹ Tamás Arányi,⁷ Robin Ketteler,⁴ Michael D. Schneider,¹ Chris Denning,³ and Sian E. Harding¹

¹National Heart and Lung Institute, Imperial College London, London W12 0NN, UK

²Heart and Vascular Center, Semmelweis University, Budapest H1122, Hungary

³Wolfson Centre for Stem Cells, Tissue Engineering and Modelling, Centre for Biomolecular Sciences, University of Nottingham, Nottingham NG7 2RD, UK

⁴Bioinformatics Image Core, Medical Research Council Laboratory for Molecular Cell Biology, University College London, London WC1E 6BT, UK

⁵Oxford Centre for Diabetes, Endocrinology, and Metabolism, Oxford University, The Churchill Hospital, Oxford OX3 7LJ, UK

⁶National Institute for Biological Standards and Controls, Cell Biology and Imaging, Hertfordshire EN6 3QG, UK

⁷Institute of Enzymology, RCNS, Hungarian Academy of Sciences, Budapest H1113, Hungary

*Correspondence: g.foldes@imperial.ac.uk

<http://dx.doi.org/10.1016/j.stemcr.2014.09.002>

This is an open access article under the CC BY-NC-ND license (<http://creativecommons.org/licenses/by-nc-nd/3.0/>).

SUMMARY

Cardiomyocytes from human embryonic stem cells (hESC-CMs) and induced pluripotent stem cells (hiPSC-CMs) represent new models for drug discovery. Although hypertrophy is a high-priority target, we found that hiPSC-CMs were systematically unresponsive to hypertrophic signals such as the α -adrenoceptor (α AR) agonist phenylephrine (PE) compared to hESC-CMs. We investigated signaling at multiple levels to understand the underlying mechanism of this differential responsiveness. The expression of the normal α_1 AR gene, *ADRA1A*, was reversibly silenced during differentiation, accompanied by *ADRA1B* upregulation in either cell type. *ADRA1B* signaling was intact in hESC-CMs, but not in hiPSC-CMs. We observed an increased tonic activity of inhibitory kinase pathways in hiPSC-CMs, and inhibition of antihypertrophic kinases revealed hypertrophic increases. There is tonic suppression of cell growth in hiPSC-CMs, but not hESC-CMs, limiting their use in investigation of hypertrophic signaling. These data raise questions regarding the hiPSC-CM as a valid model for certain aspects of cardiac disease.

INTRODUCTION

The potential of stem cell-derived cardiomyocytes for disease modeling has been enhanced by the realization that cardiomyocytes from human embryonic stem cells (hESC-CMs) and induced pluripotent stem cells (hiPSC-CMs) can be obtained also with disease-specific genotypes and phenotypes (Park et al., 2008). These cells are suggested to have many of the properties of authentic cardiomyocytes, and their phenotypes provide validation that characteristics of the disease can be reproduced in vitro (Park et al., 2008). The initial focus for using hESC-CMs or hiPSC-CMs was modeling acute cardiac responses, with the aim of producing models of contractile impairment, contractile frequency, or arrhythmias or for using cells as a screen to identify cardiotoxicity of experimental or clinical compounds. An important goal is now to extend this to modeling of longer-term disease processes. Hypertrophy is an obvious target for investigation, given its central role in the transition to heart failure. Intense studies in animal models and human myocardium have revealed hypertrophic networks with complex interdependence and redundancies (Ryall et al., 2012), which makes the design of therapies challenging. The high-throughput capabilities of the hESC-CM/hiPSC-CM system are ideally placed to dissect these pathway interactions by systems approaches

and then to translate into a drug discovery platform. Our earlier data have revealed the ability of hESC-CMs to respond to canonical pathological and physiological hypertrophic stimuli (Földes et al., 2011). In the present study, we extend these observations using newly designed assays on a number of automated platforms and show how these approaches can identify new targets. Although the field of modeling of genetic diseases has advanced rapidly, researchers have started to evaluate more critically hiPSCs relative to hESCs (Ma et al., 2014) and have made an effort to better understand how these cell populations differ from one another. We present here data showing that hiPSC-CMs diverge systematically from hESC-CMs and investigate the reason for the difference at multiple levels from receptor expression to kinase effector pathways.

RESULTS

Distinct Responses of Cardiomyocyte Derived from hESC and hiPSC Lines to Phenylephrine

The structural features of 30- to 40-day-old hESC-CMs and hiPSC-CMs (details of cell lines are in Table S1 available online) were analyzed and compared using immunocytochemistry. Cardiomyocytes differentiated from various hESCs in different laboratories or companies (H7, Imperial

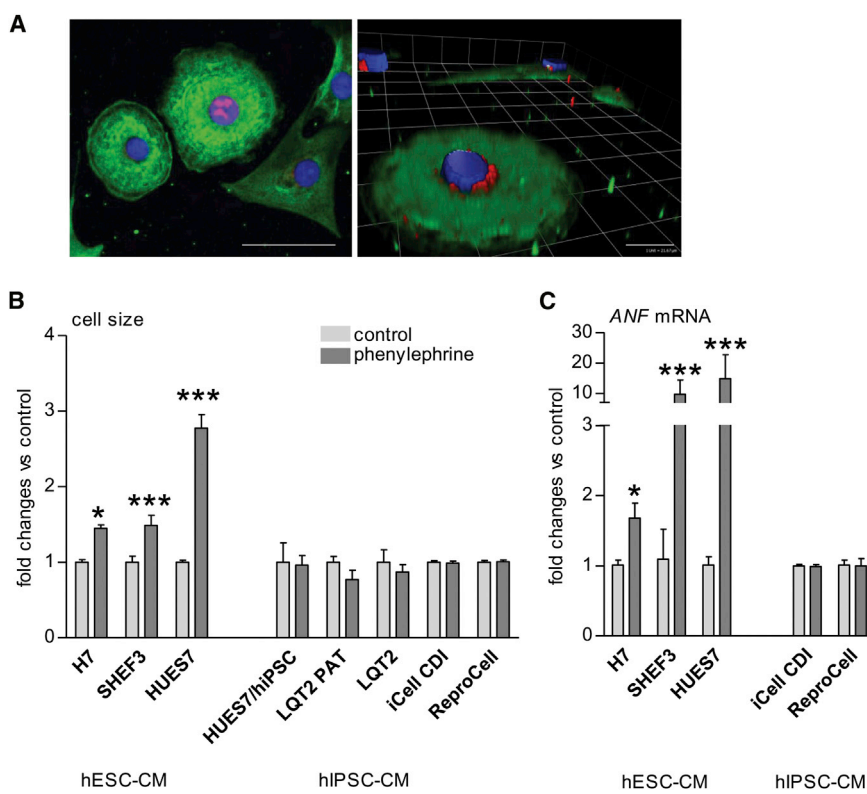


Figure 1. Distinct Responses of Cardiomyocyte Derived from hESC and hiPSC Lines to Phenylephrine

(A) Representative immunofluorescence confocal image and 3D rendering of a confocal image stack showing differentiated hiPSC-CMs stained positive for cardiac-specific myosin heavy chain α/β (green) and ANF (red) at 30 days after differentiation. Nuclei are stained with DAPI (blue). White scale bars represent 20 μ m. Cardiomyocytes differentiated from various hESC (H7, HUES7, and SHEF3) and hiPSC (LQT2, LQT2-PAT, CDI, and ReproCell) lines showed comparable morphology after plating onto 0.5% gelatine. The hESC-CMs and hiPSC-CMs were treated with phenylephrine (PE) (10 μ M, 48 hr) at 30 days after differentiation.

(B and C) Bar graphs showing fold change in 2D cell area (B) and ANF mRNA levels (C) in cells treated with pPE. Results are shown as fold changes versus control group. $n > 100$ MHC-positive cells analyzed per well (mean \pm SEM), from two to ten biological replicates. * $p < 0.05$, *** $p < 0.001$ versus control groups; Student's t test.

See also Figures S1 and S2.

College and GE Healthcare; HUES7, University of Nottingham; and SHEF3, UK Stem Cell Bank) and hiPSCs (hiPSCs reprogrammed from HUES7 hESC-derived fibroblasts, LQT2, and LQT2-PAT, University of Nottingham; iCell, Cellular Dynamics; and ReproCell) lines showed comparable morphology after plating onto 0.5% gelatine (representative cell images in Figure 1A). Specifically, hiPSC-CMs and hESC-CMs displayed structural features of the immature phenotype in terms of shape and sarcomeric pattern (Gherghiceanu et al., 2011). We investigated the effects of hypertrophic stimuli on cell area of various hESC-CM and hiPSC-CM types. Administration of phenylephrine (PE) resulted in a significant increase in cell area of hESC-CMs (H7: 1.4-fold, $p < 0.05$; SHEF3: 1.5-fold, $p < 0.05$; HUES7: 2.8-fold, $p < 0.001$ versus control; Figure 1B). In contrast, administration of PE did not change the myosin heavy chain (MHC)-labeled 2D area of hiPSC-CMs from any of the stem cell lines (LQT2, LQT2-PAT, iCell, and ReproCell hiPSC-CMs; Figure 1B). Furthermore, mRNA levels of ANF, a marker of hypertrophy, increased in various hESC-CMs while staying unchanged in hiPSC-CMs (Figure 1C). Similarly, there were no significant changes in BNP mRNA levels in response to PE (0.75 ± 0.15 as compared with control, $p = 0.29$, $n = 3$). Given the known hypertrophic effect of serum on primary rat neonatal cells, and the reported effect on hESC-CMs/hiPSC-CMs (Dambrot

et al., 2014), we compared the hESC-CMs (H7) and hiPSC-CMs (iCell) with 20% serum or no serum in the medium (RPMI/B27). High-content analyses of these did not reveal any significant differences in hypertrophic responsiveness (Figure S1).

Responses to Other Hypertrophic Agonists

Endothelin-1 increased mRNA levels of ANF both in hESC-CMs and hiPSC-CMs after 24 hr ($p < 0.01$), while the increase in cell size was small (10%, not significant) (Figure S2). Angiotensin II had no significant effect on hESC-CM and hiPSC-CM cell size and increased ANF mRNA levels only in hESC-CMs (Figure S2). Endothelin-1 at 10 nM concentration increased BNP mRNA levels in hiPSC-CMs (2.42 ± 0.16 -fold, $n = 3$, $p = 0.038$) whereas angiotensin II had no effect (0.97 ± 0.12 , $p = 0.81$, $n = 3$).

Administration of β -adrenergic agonist isoprenaline (10 μ M) alone or in combination with β_1 AR inhibitor CGP20712A (300 nM) to reveal β_2 AR effects had minimal effect on cell size in hESC-CMs or hiPSC-CMs (Figures S2E–S2G), although contractile responses to β_1 AR or β_2 AR agonists were intact.

Loss of ADRA1A Expression during Differentiation

Our data confirmed ADRA1A as the main α -adrenergic receptor isoform in adult ventricular cardiomyocytes, while

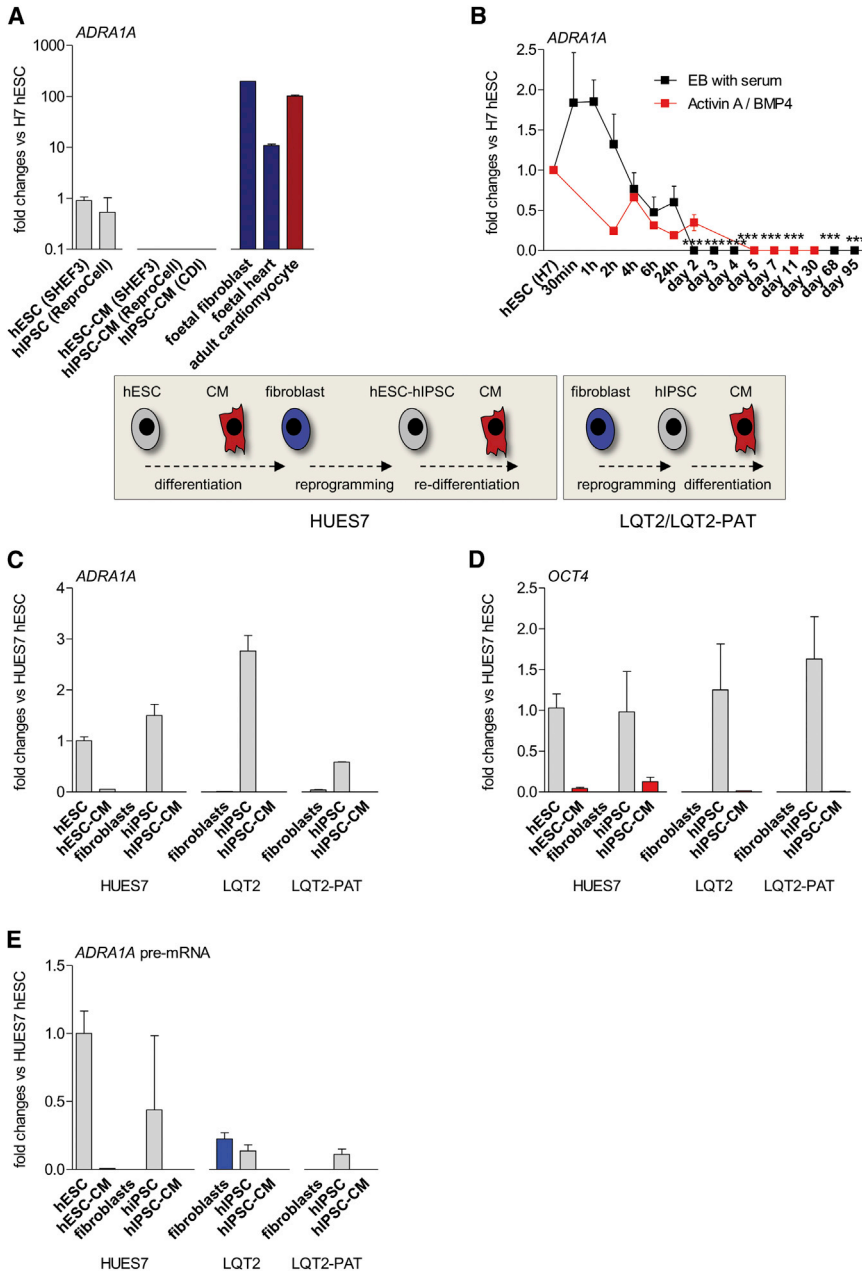


Figure 2. Silenced Expression of ADRA1A during hESC and hiPSC Differentiation toward Cardiomyocyte

(A) Bar graphs showing mRNA levels of ADRA1A in undifferentiated hESC, hiPSC, hiPSC-CM, hESC-CM, as well as adult myocytes and fetal heart and fibroblasts.

(B) Line graph showing the time course of ADRA1A downregulation during differentiation of H7 hESC by serum-free directed differentiation and serum-based EB methods (mean ± SEM; four biological replicates; ***p < 0.001 versus control groups; one-way ANOVA with Dunnett’s post hoc test).

(C–E) Diagram showing the experimental scheme of differentiation and reprogramming. Bar graphs showing ADRA1A mRNA (C), OCT4 mRNA (D), and ADRA1A pre-mRNA levels (E) in HUES7-hESC, HUES7-hiPSC, and HUES7-hiPSC-derived cardiomyocytes or fibroblasts, adult skin fibroblasts, and hiPSC- and hiPSC-derived cardiomyocytes from a patient with LQ2 syndrome and a healthy relative (LQ2-PAT).

Undifferentiated cells are shown as gray, differentiated cardiomyocytes as red, differentiated fibroblasts as blue, adult cardiomyocytes as dark red, and adult fibroblasts as dark blue bars. Results are shown as fold changes versus the undifferentiated hESC group (H7 in A and B; HUES7 in C–E, respectively); mean ± SEM. Samples were measured in triplicate from two biological replicates. See also Figure S3.

expression was much lower for ADRA1B (Figures 2A and S3A). Human fetal fibroblasts, adult heart samples, as well as isolated adult ventricular myocytes showed abundant expression of ADRA1A, suggesting a preserved dominant expression of ADRA1A during human cardiogenesis (Figure 2A). ADRA1A mRNA was present in undifferentiated hESCs and hiPSCs (although modest compared with adult cells) but was not detectable in differentiated hiPSC-CMs or hESC-CMs (Figure 2A). Prior exposure to hypertrophic effectors such as PE or endothelin-1 did not induce ADRA1A mRNA expression in hiPSC-CMs.

Expression of ADRA1A mRNA was markedly down-regulated during differentiation from all hESC and hiPSC lines we studied (Figure 2A). Downregulation was independent from reprogramming methods of hiPSC or differentiation methods (Table S1; Figure 2A). Downregulation of ADRA1A mRNA was rapid (following an early transient upregulation in ADRA1A within 2–4 hr) and was stable, as shown by long-term follow-up of differentiated hESC-CM cultures made by either the embryoid body or Activin A/BMP4 methods (Figure 2B).

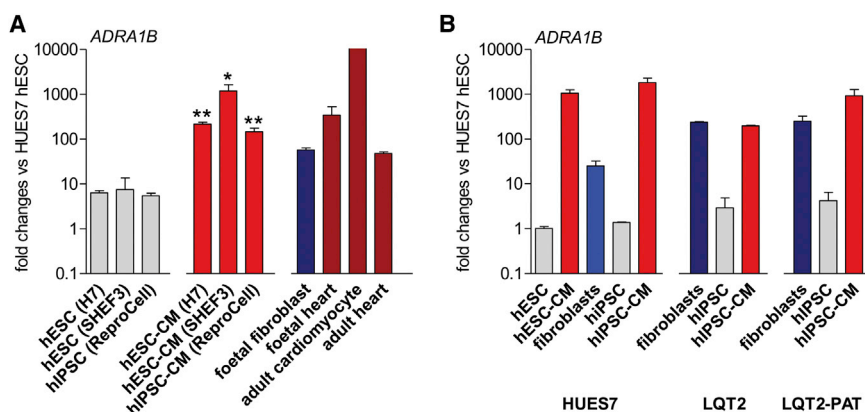


Figure 3. Upregulation of ADRA1B Expression during Differentiation of hESCs and hiPSCs

(A) Quantitative RT-PCR data on *ADRA1B* expressions in undifferentiated hESCs, hiPSCs, hiPSC-CMs, hESC-CMs, and adult myocytes isolated from the left ventricle, adult heart, and fetal heart and fibroblasts. Undifferentiated cells are shown as gray, differentiated cardiomyocytes as red, differentiated fibroblasts as blue, adult cardiomyocytes as dark red, and adult fibroblasts as dark blue bars. Data are expressed as relative changes versus DMSO-treated differentiating control hESCs or hiPSCs; mean \pm SEM, *** p <

0.001 versus undifferentiated group; Student's t test. Samples are from three biological replicates.

(B) The diagram in Figure 2 shows the experimental scheme of differentiation and reprogramming. Bar graphs showing *ADRA1B* mRNA in HUES7-hESC-, HUES7-hiPSC-, and HUES7-hiPSC-derived cardiomyocytes or fibroblasts, adult skin fibroblasts, and hiPSC- and hiPSC-derived cardiomyocytes from a patient with LQT2 syndrome and a healthy relative (LQT2-PAT) are presented. Undifferentiated cells are shown as gray, differentiated cardiomyocytes as red, differentiated fibroblasts as blue, adult cardiomyocytes as dark red, and adult fibroblasts as dark blue bars. Results are shown as fold changes versus undifferentiated hESC group; mean \pm SEM. Samples were measured in triplicate from two biological replicates.

Reprogramming of adult fibroblasts with low or no *ADRA1A* mRNA levels resulted in a considerable increase in *ADRA1A* mRNA levels in the undifferentiated state (Figure 2C) from arrhythmic patients with long QT2 syndrome or a healthy relative (LQT2-PAT). During further differentiation of the patient-derived hiPSC lines into beating cardiomyocytes, there was a silencing of *ADRA1A* expression. In both cases, *ADRA1A* levels changed in parallel with the undifferentiated pluripotent stem marker *OCT4* (Figure 2D). To further compare hESC-CMs with hiPSC-CMs in a robust system, we have also used HUES7 hESC line as a starting point (with measurable *ADRA1A* mRNA levels; Figure 2C). Differentiation of HUES7 hESCs into fibroblasts and cardiomyocytes resulted in a loss of *ADRA1A* mRNA expression. Then, we reprogrammed HUES7-derived fibroblasts into hiPSCs (HUES7-hiPSCs), which restored *ADRA1A* mRNA expression. Finally, further differentiation of HUES7-hiPSCs into cardiomyocyte cultures switched off *ADRA1A* expression (Figure 2C). Again, changes in mRNA levels of marker *OCT4* were parallel to those of *ADRA1A* in all samples (Figure 2D). We measured changes in pre-mRNA levels of *ADRA1A* by intron-specific real-time PCR primers to reflect changes in gene transcription rates in addition to measurements of mRNA levels by exonic probes (Figure 2E). Changes in pre-mRNA levels were parallel with exon-specific profile, suggesting that these together may mainly reflect changes in *ADRA1A* gene transcription rate in the differentiated cardiomyocytes and pluripotent stem cells (Ponzio et al., 2007).

Coregulation of the α_{1B} -Adrenergic Receptor

Since the α_1 AR was lost in both hESC-CMs and hiPSC-CMs, this left the question of why the hESC-CMs were still able to respond to PE. It is known that there are other subtypes of the α_1 AR, and that α_{1B} AR can also support the hypertrophic response (O'Connell et al., 2003). In contrast to *ADRA1A*, expression of *ADRA1B* showed marked upregulation during differentiation of hESCs or hiPSCs toward cardiomyocytes (and fibroblasts), bringing expression levels to those of adult cells (Figure 3A). This was reversible by reprogramming fibroblasts into undifferentiated hiPSCs (Figure 3B) (Ponzio et al., 2007).

Rescue of ADRA1A Did Not Restore Responsiveness to PE

We overexpressed *ADRA1A* in hiPSC-CMs, resulting 10,000-fold increase in *ADRA1A* expression, reaching a comparable level to those in adult cardiomyocytes (Figures 4A and 4B). *ADRA1A* was widely spread, with an apparent strong localization on microtubule network as well as close to the membrane and nucleus (Figure 4A). However, cell size and atrial natriuretic factor (ANF) mRNA levels did not change in response to PE in hiPSC-CMs with high *ADRA1A* levels (Figures 4C and 4D), suggesting changes in downstream signaling were additionally preventing hypertrophy.

Distinct Expression of Downstream G Proteins during Differentiation

Downstream partners of adrenergic signaling including Gq, G β 1, and G γ 2 proteins were all detectable in various

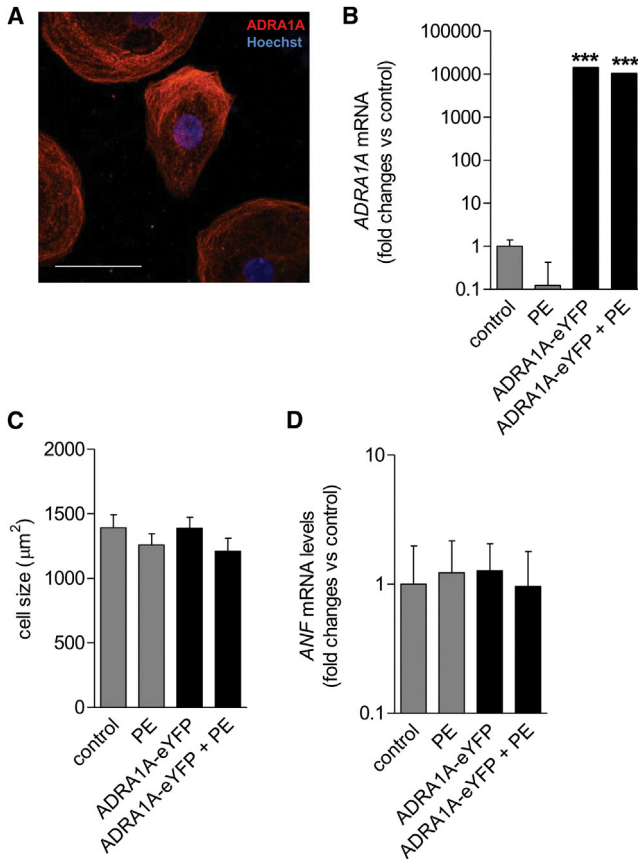


Figure 4. Overexpression of ADRA1A in hiPSC-CM

(A) Localization of ADRA1A in hiPSC-CM (iCell) transfected with ADRA1A-eYFP construct. White scale bar represents 20 μ m. (B–D) Bar graphs showing *ADRA1A* mRNA levels (B), cell size (C), and *ANF* mRNA levels (D) in hiPSC-CMs transfected with ADRA1A without or in the presence of PE after 48 hr; mean \pm SEM; six biological replicates. *** p < 0.001 versus control group; one-way ANOVA with Tukey's post hoc test.

lines of undifferentiated hESCs/hiPSCs, fetal hearts and fibroblasts, and adult ventricular cardiomyocytes (Figures 5A–5C). Our data show an increase in *Gq*, *G β 1*, and *G γ 2* mRNA levels during cardiac differentiation in hESC differentiation. In contrast, in most differentiating hiPSC lines, mRNA levels of *Gq*, *G β 1*, and *G γ 2* were unchanged or downregulated during differentiation, suggesting a distinct regulation of downstream signaling elements (Figures 5D–5F).

Distinct α_{1B} AR-Adrenergic Receptor-Dependent Kinase Pathways in hESC-CMs and hiPSC-CMs

We assessed downstream signaling pathways using proteome screening for kinase phosphorylation. Despite the lack of functional responses in hypertrophy-related parameters, evidence of active signaling was seen in hiPSC-CMs,

as well as the expected effects in hESC-CMs. Phosphorylation of src family members Lck (Y394), Yes (Y426), Fgr (Y412), Chk2 (T68), and Pyk2 (Y402) was markedly increased in response to PE after 48 hr in both cell types (Figure 6A). In some aspects, hiPSC-CMs were more affected than hESC-CMs; there was activation of STAT3 (Y705), STAT5a/b (Y694/699), and STAT6 (Y641) as well as of β -catenin and GSK3 α/β (S21/59) and GSK3 β /Wnt-pathway elements, while phosphorylation levels of these kinases were unchanged or decreased in hESC-CMs in response to PE (Figure 6A). For RSK, Pyk2, P70 S6, and p27, the opposite pattern was seen, with increased phosphoprotein in hESC-CMs but unchanged or decreased phosphoprotein in hiPSC-CMs. Connections between the kinases were explored by Ingenuity Pathway Analysis, and a schematic diagram showed how STAT3, which is an established ADRA1B downstream target (Han et al., 2008), could produce the phosphorylation changes observed in an EGFRK/Src/GSK3 β network (Figure 6B).

Inducing Cell Growth in hiPSC-CMs by Kinase Inhibition/Activation

Our previous study had identified protein kinase pathways (mTOR and ERK1/2) that regulate PE-induced changes cell area and ANF expression in hESC-CMs (Földes et al., 2011), and this was confirmed here (Figure 6C). Here we used these methods for a comparison between hESC-CM and hiPSC-CM, with newly developed assays for 2D and 3D automated microscopy and an extended library of inhibitors. Unexpectedly, given the lack of increase in cell area with PE in hiPSC-CMs, the same kinase inhibitors decreased cell area in those cells also (Figure 6C). This suggests that these pathways are active in maintaining cell size in both cell types, but there may be additional mechanisms in hiPSC-CMs that are producing a tonic suppression of the hypertrophic response to PE. Given the implication that ADRA1B might stimulate hypertrophy through a STAT3 cascade, inhibitors and activators of STAT3 were tested in hESC-CMs and hiPSC-CMs. STAT3 inhibitor VIII, 5,15-DPP was able to block PE-induced increase in cell size of hESC-CMs as well as decrease basal cell size in both cell types. We observed a similar tendency with cell-permeable STAT3 inhibitor protein. However, STAT3 inhibitor protein had no effect on hiPSC-CMs (iCell, from CDI) (Figures S4A and S4B). Conversely, the STAT3 agonist interleukin-6 (IL-6), while ineffective alone, rescued a strongly hypertrophic effect of PE on cell area in hiPSC-CM (Figures 6D–6F).

Interestingly, translocation assays of STAT3 to the nucleus showed the movement to be induced by PE alone, which had no hypertrophic effect, as well PE + IL-6, which did, further supporting the idea of active hypertrophic signaling by PE in hiPSC-CMs suppressed by additional pathways (Figure 6E). To investigate this further, we used

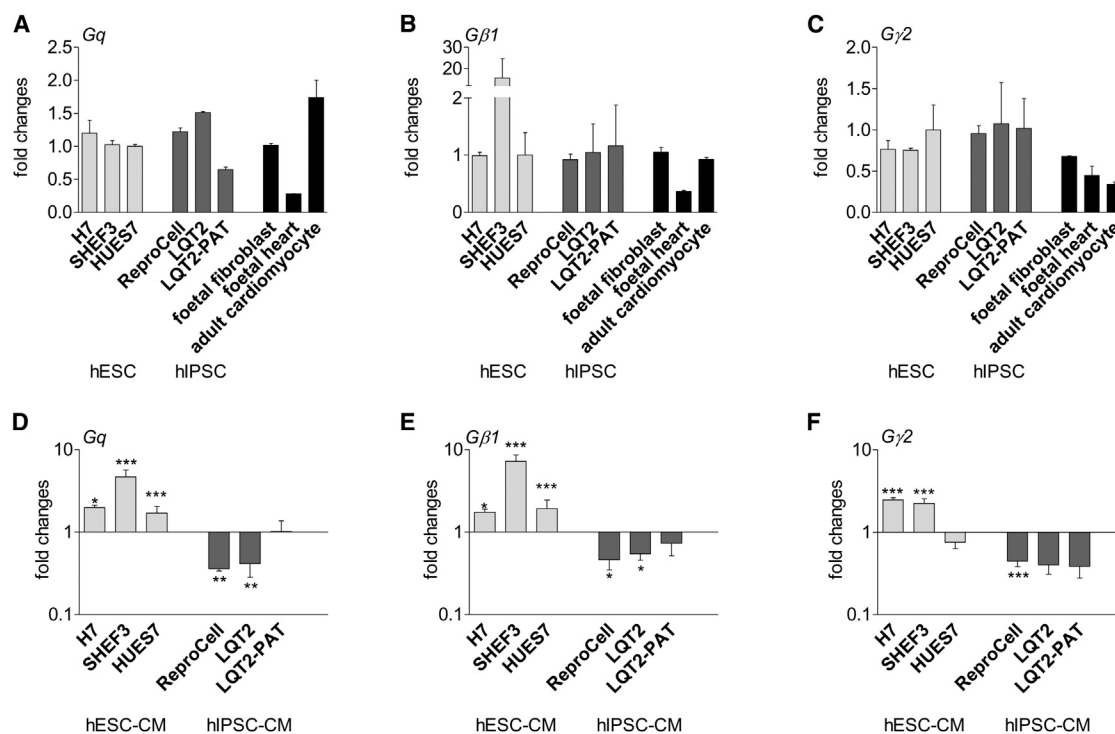


Figure 5. Distinct Expressions of Downstream G Protein during Differentiation from hESCs and hiPSCs toward hESC-CMs and hiPSC-CMs

(A–C) mRNA for *Gq* (A), *Gβ1* (B), and *Gγ2* (C) proteins were all detectable in various lines of undifferentiated hESC (light gray bars) and hiPSC (dark gray bars) cultures, fetal hearts, and fibroblasts and adult ventricular cardiomyocytes from heart failure patients (black bars). Results are shown as fold changes versus the undifferentiated hESC (HUES7) group (mean \pm SEM; three biological replicates).

(D–F) Changes in mRNA levels for *Gq* (D), *Gβ1* (E), and *Gγ2* (F) during differentiation of hESCs or hiPSCs are also presented. Results are shown as fold changes versus the respective undifferentiated hESC or hiPSC line. Samples were measured in triplicate from three biological replicates. * $p < 0.05$, ** $p < 0.001$; Student's t test.

a panel of inhibitors of components identified in the phosphoproteome network above (Figure 6B). GSK3 β and (in some cases) EGFRK had different effects between PE-treated hESC-CMs and hiPSC-CMs in the control of cell area (Figure 6C), volume (Figures S5A and S5B), sarcomere organization (Figures S5A and S5C) and/or ANF subcellular distribution (Figures S5A and S5D). Simultaneously targeting these kinases with a combination of GSK3 β , EGFRK, and CAMKII inhibitors had an inducer effect on cell growth (Figure 6G).

DISCUSSION

α -Adrenergic receptors play a critical role in the regulation of cellular growth pathways, including hypertrophy and proliferation. G protein-coupled α_1 ARs are the predominant α -adrenergic subtype in the myocardium of most species (Brückner et al., 1985), and catecholamine receptor agonists strongly induce pathological cardiac hypertrophy both in vivo and in vitro (Zhong and Minneman, 1999; Rokosh et al., 1996). Development of model systems have

therefore focused on the response through the α_1 AR as a means to understand the downstream signaling involved and to develop therapeutic agents against hypertrophic conditions. Expression of *ADRA1A* subtype mRNAs is tissue and cell specific (Stewart et al., 1994), and control of *ADRA1* mRNAs by agonists can be also diverse in different cells (Rokosh et al., 1996). It is therefore crucial that the new hESC-CMs and hiPSC-CMs are characterized with respect to their α_1 AR repertoire. We had previously seen robust and specific effects of the canonical α_1 AR agonist PE on a wide range of markers of hypertrophy such as cell size, cell volume, ANF expression, sarcomere alignment, and protein/DNA ratio (Földes et al., 2011). While these observations were confirmed here in an hESC-CM from a number of lines, surprisingly we found that hiPSC-CM were in contrast unresponsive to PE. Loss of PE response was independent from the cell line, cell culture conditions, reprogramming, and differentiating protocols we used and was reproduced in different laboratories.

Our data confirm that α_{1A} AR (*ADRA1A* gene) is the dominant receptor subtype of the α_1 AR expressed in the

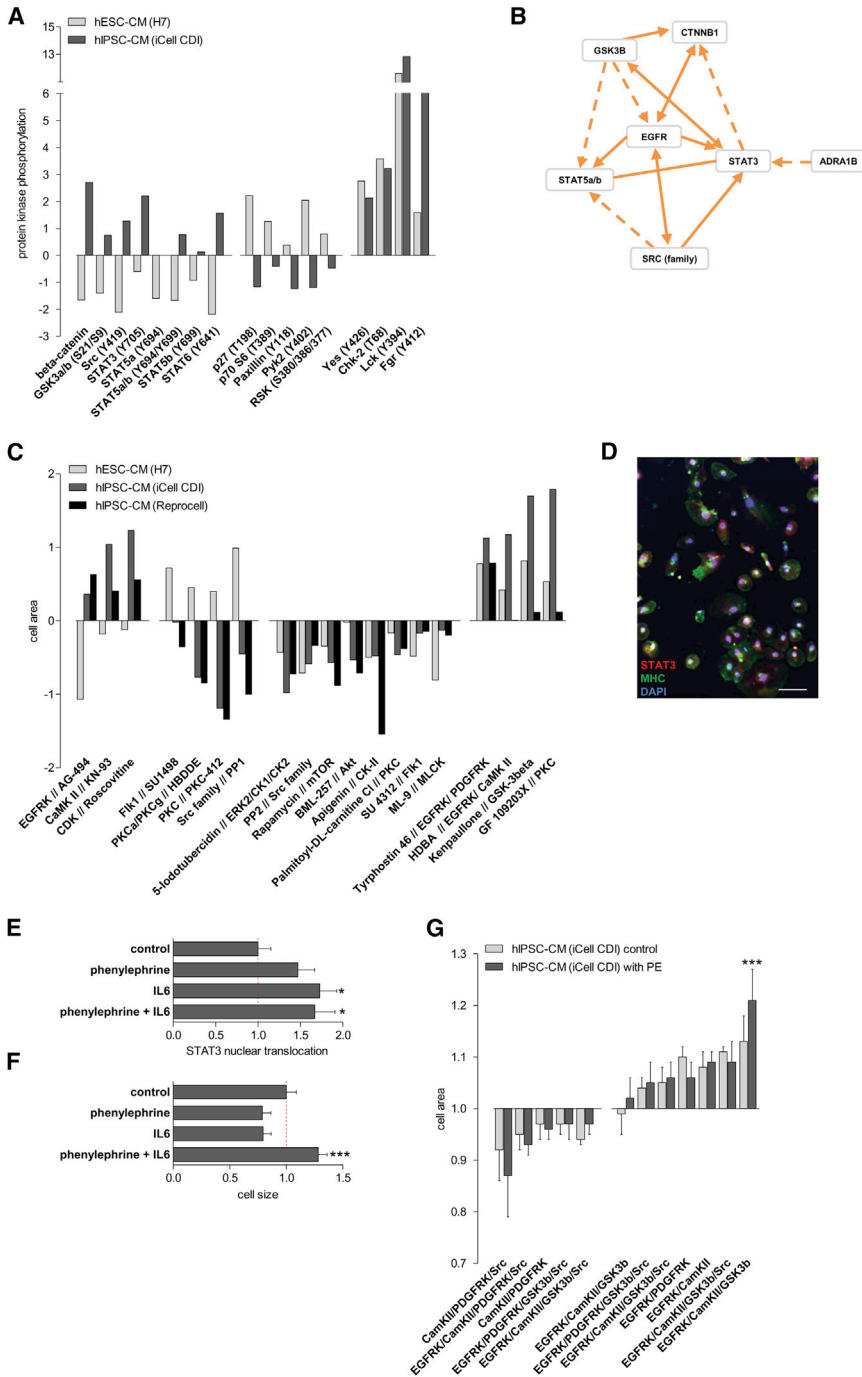


Figure 6. Phosphokinase Proteome and Kinase Inhibitor Analyses of PE-Induced Signaling in hESC-CMs and hiPSC-CMs

(A) Relative changes in phosphoprotein levels in response to PE (10 μ M, 48 hr) in hESC-CMs (H7) and hiPSC-CMs (iCell).

(B) Schematic diagram of Ingenuity Pathway Analysis-mapped mechanistic interactions of active epidermal growth factor receptor kinase, STAT family members, and GSK3 β / β -catenin and Src kinase pathways. Arrows between nodes represent direct (solid lines) and indirect (dashed lines) interactions between molecules as supported by information in the Ingenuity Pathway Knowledge Base.

(C) Assessment of kinase inhibitors on hypertrophy. Human ESC-CMs (H7) and hiPSC-CMs (iCell and ReproCell) were treated with PE in the presence of kinase inhibitors. Bar graphs show changes in response to selected kinase inhibitors on cell area by automated high-content microscopy. Robust Z score was computed and visualized.

(D–F) Representative image and quantitation of nuclear translocation of STAT3 (D and E) and cell area (F) in hiPSC-CMs treated with PE in the presence of interleukin-6 (100 ng/ml) in hiPSC-CMs. White scale bar represents 20 μ m.

(G) Cell area in hiPSC-CMs treated with PE in the presence of combined inhibition of GSK3 β /EGFRK/CAMKII/src/PDGFRK (1 μ M each); mean \pm SEM; four biological replicates; one-way ANOVA with Tukey's post hoc test.

See also Figures S4 and S5.

human adult heart and ventricular myocytes. However, cardiomyocytes differentiated from hESCs or hiPSCs did not measurably express the *ADRA1A* gene. *ADRA1A* mRNA was expressed (albeit modestly) in undifferentiated hESCs and hiPSCs but disappeared rapidly during differentiation to either cardiomyocytes or fibroblasts. There was a close correspondence between loss of pluripotency genes and loss of the *ADRA1A* receptor. Once again, this

was independent of line or reprogramming method; in our definitive experiment, we showed this by reprogramming fibroblasts differentiated from an hESC line and comparing the resulting hiPSC-CMs with the hESC-CMs from the same line. Since loss of the α_{1A} AR occurred in both hESC-CMs and hiPSC-CMs, we were now left with the conundrum of why there was an active PE response in hESC-CMs and why the two cell types differed. We



further explored alternate α AR subtypes and showed that differentiation activated a unique, nonontogenetic gene program by a marked shift from ADRA1A toward a dominant ADRA1B subtype both in hiPSC-CMs and hESC-CMs. However, expression levels of *ADRA1B* were considerably increased in both cell types, which again did not explain the difference between hiPSC-CMs and hESC-CMs. Other subtypes (ADRA1D or ADRA2C) are also present both in hiPSC-CMs and hESC-CMs. However, lack of hypertrophic responsiveness to PE suggests that their presence is not sufficient to mediate PE effects in hiPSC-CMs.

We then attempted to restore the response to PE by overexpression of ADRA1A, but this too was unsuccessful despite high levels of receptor expression. This strongly suggests that there is either loss of coupling components for the downstream signaling pathway or active repression of hypertrophy by opposing signaling pathways. The next level of regulation for the α_1 AR is at the G protein-coupling stage, with agonist binding to the receptor allowing activation of the *G α q* subunit by dissociation from *G β γ* proteins. While levels of *G α q*, *G β* , and *G γ* were similar between undifferentiated hESCs and hiPSCs (and also similar to adult cardiomyocytes), differences then occurred during differentiation. We found an increase in *Gq*, *G β 1*, and *G γ 2* mRNA levels during hESC differentiation, whereas in most differentiating hiPSC lines, the mRNA levels were unchanged or downregulated. This represents a clear difference between the two cell types and would be expected to produce a relative damping of the hypertrophic response in hiPSC-CMs. However, other Gq-coupled hypertrophic agents (ET-1 and angiotensin II) produced only small changes in cell size in either cell type, but robust increases in ANF and B-type natriuretic peptide (BNP) were observed even in hiPSC-CMs. This suggests that G protein coupling is not entirely compromised in these cells. Increases in cell size somewhat larger than this have been reported for iCell hiPSC-CMs with ET-1 (24% versus our 10%) (Carlson et al., 2013), but it is notable that the stronger BNP signal was chosen for the final hypertrophy assay in that study, which would be consistent with our findings.

We next used the high-content imaging to further define hypertrophic pathway interactions in hESC-CMs and hiPSC-CMs and to compare this with data defining the phosphorylation effects of PE treatment. We have developed 2D and 3D imaging processes to analyze hypertrophic phenotype of our cells using high-content analysis, and we used these while extending our original panel of kinase inhibitors (Földes et al., 2011) to cover many pivotal kinase targets. This is an important advance on our previous experiments, where we used a limited panel, because few inhibitors are completely specific. In Figures 6C and S5, the

abscissa titles show that many inhibitors have multiple targets; bioinformatic analysis was therefore necessary to deconvolve the pathways clusters involved. Although the positive effect of PE on hypertrophic markers was not evident in hiPSC-CMs, we were surprised to see negative effects of kinase inhibitors on a number of parameters. These included the original p38-MAPK, ERK1/2, and mTOR inhibitors that were effective in hESC-CMs (in both this and our previous study; Földes et al., 2011). Some inhibitors, such as those for GSK3 β and EGFRK, were also able to increase cell size and area, suggesting that there had been tonic suppression of cell growth by these pathways. We also noted a number of clear differences between hESC-CM and hiPSC-CM responses, such as an increase of cell volume in hiPSC-CMs, but not hESC-CMs, with inhibitors of EGFRK or the STAT activator JAK-2. This suggests a greater tonic suppression of ADRA1B hypertrophic signaling in the hiPSC-CM, which would again contribute to the poor responses to PE.

Detection of PE-dependent phosphorylation of the kinases themselves with a proteome profiling array showed that Src family kinases, a nonreceptor tyrosine kinase group implicated in controlling G protein-coupled receptor trafficking and effects on cell proliferation and cytoskeletal rearrangement, were markedly activated in hESC-CMs and hiPSC-CMs. The Ingenuity Pathway Analysis identified an EGFR/Src/GSK3 β /STAT3 network modulated by ADRA1B that could drive the hypertrophic process. STAT3 is an established ADRA1B downstream target (Han et al., 2008), and the finding is in line with previous reports of activation of Src-dependent pathways by ADRA1 and crosstalk between EGF signaling and ADRA1 in cardiac hypertrophy (Li et al., 2011; Zitron et al., 2008; Asakura et al., 2002). Supporting this schema, a STAT3 inhibitor was able to reduce both basal and PE-stimulated cell area in the hESC-CMs as well as basal in hiPSC-CMs. Also, a STAT activator (IL-6) caused a marked increase in PE-stimulated cell area in the hiPSC-CMs. PE was able to induce STAT3 movement to the nucleus, but it was only able to increase cell area in the presence of IL-6. The simultaneous activation of EGFRK/GSK3 β by PE via STAT3 may have restrained the final cell size change following translocation. A smaller panel of inhibitors, based on the array above, was used in combination to identify the antihypertrophic pathways most active in the hiPSC-CMs. This confirmed the EGFRK/GSK3 β combination, together with CamKII, as optimal to increase cell area.

We conclude that the main difference in hiPSC-CMs that accounts for the defective response to α_1 AR stimulation is the suppression of growth by tonic antihypertrophic pathways (Figure 7), including EGFRK, GSK3 β , and CamKII. The limitations of this study are that this screen is not fully comprehensive, and so we may have missed

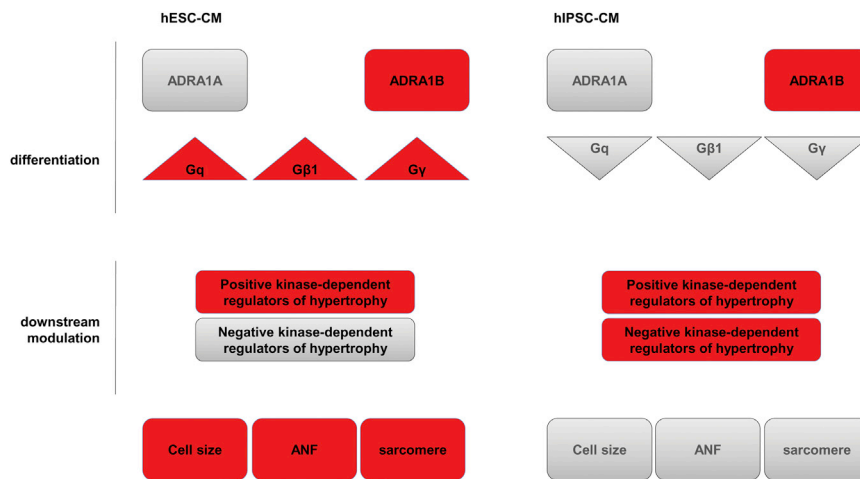


Figure 7. Schematic Summary of Potential Differences in Adrenergic Receptor-Driven Regulation of Cell Growth and Hypertrophy in hiPSC-CMs and hESC-CMs Red is used to represent active/upregulated components and gray for relatively inactive or downregulated components.

other elements and combinations that could have further rescued hypertrophy in hiPSC-CMs. Nor can we say that this will be predictive of every hiPSC-CM line, since we have not identified the genetic or epigenetic change produced by the reprogramming process, which may have triggered the different balancing of hypertrophic/antihypertrophic pathways. We further note that even in hESC-CMs, where α_1 AR-mediated cell size increases are clear, there has been a differentiation-induced shift in the α AR subtype. These data send an important message that superficial similarities in phenotype between cardiomyocytes derived from hESCs or hiPSCs, and parallels to adult cardiomyocytes, may mask complex differences in signaling. This has implications for their use in drug discovery, where targets identified using pluripotent stem cell derivative may not ultimately act in the same way in adult human cardiac cells.

EXPERIMENTAL PROCEDURES

Human Pluripotent Stem Cell-Derived Cardiomyocytes

Cardiomyocytes derived from hESC and hiPSC lines were generated from dense monolayers with Activin A and bone morphogenetic protein 4 (BMP4) or by using the embryoid body (EB) differentiating system. Protocols for hiPSC reprogramming and cardiomyocyte differentiation of each line are summarized in Table S1.

Use of Hypertrophic Stimuli

In vitro assays and cell lines to analyze hypertrophic responsiveness are listed in Table S2. To determine the effect of hypertrophic G protein-coupled receptor agonist, after incubation for 1 hr, plates were treated with the prohypertrophic α -adrenoceptor agonist PE (10 μ M, Sigma) or vehicle for 48 hr. For iCell hiPSC-CMs and H7 hESC-CMs, the experiments were repeated in serum-free medium and in the presence of 20% fetal

bovine serum (Dambrot et al., 2014). In a separate set of experiments, cells were also treated with angiotensin II (Sigma; 100 nM), the β -adrenergic agonist isoprenaline (Sigma; 10 μ M) with or without selective beta1 blocker CGP20712A (Sigma; 300 nM) for 48 hr, or endothelin1 (Sigma; 1, 10, and 100 nM) for 24 hr.

High-Content Imaging for Hypertrophy Assessment

We have developed high-content immunocytochemistry assays to characterize hypertrophic properties of hESC-CMs and hiPSC-CMs in culture. Cells were scanned on ArrayScan VTi 2D automated microscopy (Cellomics) and a confocal Opera LX plate reader (PerkinElmer).

Real-Time PCR for G Protein-Coupled Receptors and Downstream Signaling

Real-time PCR analyses were performed with TaqMan Gene Expression Assays on samples from undifferentiated and differentiated hESC and hiPSC cultures, adult isolated myocytes, and fetal heart and fibroblast.

Kinase Inhibitor Screen

Using BioMol Screen-Well Kinase Inhibitor Library, we assessed the role of protein kinases on basal and PE-induced changes in hypertrophy readouts.

Phosphokinase Assay

hESC-CMs and hiPSC-CMs were seeded in six-well plates and treated with PE (10 μ M) for 48 hr. Screening for different phosphokinases in cell lysates was performed with a human phosphokinase antibody array (R&D Systems). Pathway analysis was performed by Ingenuity Pathway Analysis.

Statistical Analysis

Results are expressed as mean \pm SEM. The data were analyzed by unpaired Student's t test or one-way analysis of variance and Tukey's post hoc test for multiple comparisons. Differences at the level of $p < 0.05$ were considered statistically significant.



SUPPLEMENTAL INFORMATION

Supplemental Information includes Supplemental Experimental Procedures, six figures, and two tables and can be found with this article online at <http://dx.doi.org/10.1016/j.stemcr.2014.09.002>.

ACKNOWLEDGMENTS

This paper is dedicated to the memory of Yasuyuki Asai, who died in December 2012. The ReproCell hiPSC line used in these studies was donated by ReproCell Japan under a collaborative agreement without further financial benefit to the authors. We gratefully acknowledge funding support from Foundation Leducq (G.F. and S.E.H.), the British Heart Foundation (C.D., M.D.S. and S.E.H.), the Medical Research Council (R.K., J.K.V., C.D., and S.E.H.), the NC3Rs (M.M.), a Marie Curie Reintegration grant (FP7/2007-2013, n°PIRG08-GA-2010-276811, J.K.V.), and OTKA (105555, G.F.; K100638, T.A.). T.A. is an RBUCE/UP-senior and Marie Curie fellow. K.V. is a Marie Curie fellow.

Received: January 21, 2014

Revised: August 28, 2014

Accepted: September 1, 2014

Published: October 9, 2014

REFERENCES

- Asakura, M., Kitakaze, M., Takashima, S., Liao, Y., Ishikura, F., Yoshinaka, T., Ohmoto, H., Node, K., Yoshino, K., Ishiguro, H., et al. (2002). Cardiac hypertrophy is inhibited by antagonism of ADAM12 processing of HB-EGF: metalloproteinase inhibitors as a new therapy. *Nat. Med.* **8**, 35–40.
- Brückner, R., Mügge, A., and Scholz, H. (1985). Existence and functional role of alpha 1-adrenoceptors in the mammalian heart. *J. Mol. Cell. Cardiol.* **17**, 639–645.
- Carlson, C., Koonce, C., Aoyama, N., Einhorn, S., Fiene, S., Thompson, A., Swanson, B., Anson, B., and Kattman, S. (2013). Phenotypic screening with human iPS cell-derived cardiomyocytes: HTS-compatible assays for interrogating cardiac hypertrophy. *J. Biomol. Screen.* **18**, 1203–1211.
- Dambrot, C., Braam, S.R., Tertoolen, L.G., Birket, M., Atsma, D.E., and Mummery, C.L. (2014). Serum supplemented culture medium masks hypertrophic phenotypes in human pluripotent stem cell derived cardiomyocytes. *J. Cell. Mol. Med.* **18**, 1509–1518.
- Földes, G., Mioulane, M., Wright, J.S., Liu, A.Q., Novak, P., Merkely, B., Gorelik, J., Schneider, M.D., Ali, N.N., and Harding, S.E. (2011). Modulation of human embryonic stem cell-derived cardiomyocyte growth: a testbed for studying human cardiac hypertrophy? *J. Mol. Cell. Cardiol.* **50**, 367–376.
- Gherghiceanu, M., Barad, L., Novak, A., Reiter, I., Itskovitz-Eldor, J., Binah, O., and Popescu, L.M. (2011). Cardiomyocytes derived from human embryonic and induced pluripotent stem cells: comparative ultrastructure. *J. Cell. Mol. Med.* **15**, 2539–2551.
- Han, C., Bowen, W.C., Michalopoulos, G.K., and Wu, T. (2008). Alpha-1 adrenergic receptor transactivates signal transducer and activator of transcription-3 (Stat3) through activation of Src and epidermal growth factor receptor (EGFR) in hepatocytes. *J. Cell. Physiol.* **216**, 486–497.
- Li, Y., Zhang, H., Liao, W., Song, Y., Ma, X., Chen, C., Lu, Z., Li, Z., and Zhang, Y. (2011). Transactivated EGFR mediates α_1 -AR-induced STAT3 activation and cardiac hypertrophy. *Am. J. Physiol. Heart Circ. Physiol.* **301**, H1941–H1951.
- Ma, H., Morey, R., O'Neil, R.C., He, Y., Daughtry, B., Schultz, M.D., Hariharan, M., Nery, J.R., Castanon, R., Sabatini, K., et al. (2014). Abnormalities in human pluripotent cells due to reprogramming mechanisms. *Nature* **511**, 177–183.
- O'Connell, T.D., Ishizaka, S., Nakamura, A., Swigart, P.M., Rodrigo, M.C., Simpson, G.L., Cotecchia, S., Rokosh, D.G., Grossman, W., Foster, E., and Simpson, P.C. (2003). The alpha(1A/C)- and alpha(1B)-adrenergic receptors are required for physiological cardiac hypertrophy in the double-knockout mouse. *J. Clin. Invest.* **111**, 1783–1791.
- Park, I.H., Arora, N., Huo, H., Maherali, N., Ahfeldt, T., Shimamura, A., Lensch, M.W., Cowan, C., Hochedlinger, K., and Daley, G.Q. (2008). Disease-specific induced pluripotent stem cells. *Cell* **134**, 877–886.
- Ponzio, T.A., Yue, C., and Gainer, H. (2007). An intron-based real-time PCR method for measuring vasopressin gene transcription. *J. Neurosci. Methods* **164**, 149–154.
- Rokosh, D.G., Stewart, A.F., Chang, K.C., Bailey, B.A., Karliner, J.S., Camacho, S.A., Long, C.S., and Simpson, P.C. (1996). Alpha1-adrenergic receptor subtype mRNAs are differentially regulated by alpha1-adrenergic and other hypertrophic stimuli in cardiac myocytes in culture and in vivo. Repression of alpha1B and alpha1D but induction of alpha1C. *J. Biol. Chem.* **271**, 5839–5843.
- Ryall, K.A., Holland, D.O., Delaney, K.A., Kraeutler, M.J., Parker, A.J., and Saucerman, J.J. (2012). Network reconstruction and systems analysis of cardiac myocyte hypertrophy signaling. *J. Biol. Chem.* **287**, 42259–42268.
- Stewart, A.F., Rokosh, D.G., Bailey, B.A., Karns, L.R., Chang, K.C., Long, C.S., Kariya, K., and Simpson, P.C. (1994). Cloning of the rat alpha 1C-adrenergic receptor from cardiac myocytes. alpha 1C, alpha 1B, and alpha 1D mRNAs are present in cardiac myocytes but not in cardiac fibroblasts. *Circ. Res.* **75**, 796–802.
- Zhong, H., and Minneman, K.P. (1999). Alpha1-adrenoceptor subtypes. *Eur. J. Pharmacol.* **375**, 261–276.
- Zitron, E., Günth, M., Scherer, D., Kiesecker, C., Kulzer, M., Bloehs, R., Scholz, E.P., Thomas, D., Weidenhammer, C., Kathöfer, S., et al. (2008). Kir2.x inward rectifier potassium channels are differentially regulated by adrenergic alpha1A receptors. *J. Mol. Cell. Cardiol.* **44**, 84–94.